Paper
Int'l J. of Aeronautical & Space Sci. 16(4), 485–492 (2015)
DOI: http://dx.doi.org/10.5139/IJASS.2015.16.4.485

IJASS
International Journal of Aeronautical and Space Sciences

Performance of Contra-Rotating Propellers for Stratospheric Airships

Zhihao Tang* and Peiqing Liu**

School of Aeronautic Science and Engineering, Beihang University, Beijing 100191, China

Jingwei Sun***

China Academy of Aerospace Aerodynamics, Beijing, China

Yaxi Chen**, Hao Guo***** and Guangchao Li********

School of Aeronautic Science and Engineering, Beihang University, Beijing 100191, China

Abstract

Small advance ratio and low Reynolds number of stratospheric propulsion system bring lots of challenges to the design of propellers. Contra-rotating propeller configuration is proposed to improve the propulsion efficiency. In this paper, the feasibility of contra-rotating propeller for stratospheric airship has been assessed and its performance has been investigated by wind tunnel tests. The experimental results indicate, at relatively low Reynolds number, although the advance ratio is fixed, the performance of propellers is different with variation of Reynolds number. Moreover, at the same Reynolds number, the efficiency of contra-rotating propeller achieved appears to be a few percent greater than that for a standard conventional propulsion system. It can be concluded that contra-rotating propellers would be an efficient means to improve the performance of stratospheric airship propulsion system.

Key words: contra-rotating propeller, stratospheric airship, low Reynolds number, small advance ratio

1. Introduction

There is growing worldwide interest in using airships as platforms operating for extended periods of time at very high altitudes (between 20 and 50 km) to accomplish both military and commercial missions [1-4]. The main advantages of high altitude airships rely on a high-efficiency propulsion plant. The propeller propulsion seems to be the most suitable [5]. However, lots of difficulties have been found in propeller design in research of high altitude airship propulsion system. For example, the stratospheric airships (operating at 20 km) have very slow advance speed which results in the small advance ratio (usually less than 1.5). In addition, the air condition at high altitude is significantly different from low altitude (under 10 km), such as much lower air density, which leads to extremely low Reynolds number of flow around propeller blades. These two aspects make the propellers on stratospheric airships less efficient than that on other conventional aircraft.

In this case, contra-rotating propeller (CRP) configuration may be a feasible option to improve the efficiency of stratospheric airship propulsion system based on previous investigations. For example, Biermann and Gray (1942) [6] conducted a large scale of wind tunnel experiments on CRPs whichever were tractor or pusher configurations. The results shown an 8% to 16% increase in efficiency of the CRP installed on an appropriate position. At lower advance ratio (about 3.0), the efficiency of CRPs was also found significantly improved through some further wind tunnel tests conducted by Biermann and Hartman (1942) [7]. Colehour and Davenport (1985) [8] proved that an 8% increase in efficiency of CRPs also could be gained when

* Ph.D. Student, tzh@buaa.edu.cn
** Professor, lpq@buaa.edu.cn
*** Assistant Engineer
**** Master Student
***** Assistant Professor, Corresponding Author: guohao@buaa.edu.cn
****** Assistant Professor

Received: March 16 , 2015 Revised: December 4, 2015 Accepted: December 16, 2015

Mach number is nearly 0.7. A similar conclusion was also found for high-speed transports aircrafts by Wainauski and Vaczy (1986) [9]. All the conclusions proved the prospective benefits of stratospheric airship CRPs. Futhermore, the research conducted by McHugh and Pepper (1942) [10] indicated that aerodynamically improved airfoil designs were highly related to the performance of CRPs. Gray (1944) [11] also found that the overall efficiency of a CRP was not seriously affected by small changes in blade angle or changes in rotational velocity of the rear propeller in his other researches. After 1990s, some detailed experimental investigation conducted by using advanced instruments. The three-dimensional flowfield of rotor-rotor interaction of counter-rotating fans was measured by Shin, Whitfield, and Wisler (1994) [12] using three-dimensional hot-wire anemometry. Some other experimental investigations of the complex flowfield of a generic contrarotating open rotor model at wind-tunnel scale were conducted by Sturmer (2012) [13] using particle image velocimetry (PIV) apparatus.

Unfortunately, almost all investigations of CRPs were focused on conventional aircraft at relatively low altitude and few of them aimed at application to the circumstance of low Reynolds number and small advance ratio. Therefore, in this paper, the feasibility of CRPs for stratospheric airships has been assessed and the performance of a given CRP at low Reynolds number and small advance ratio has been investigated.

2. Experimental Setup and Facilities

The experiment was conducted in Rotating Machinery Laboratory which was located in Institute of Fluid Mechanics in Beihang University. A low-speed low-turbulence open circuit wind tunnel was used. The open test section had 1.0 m in diameter. The tested CRP model had a diameter of 0.75 m which was considered as the accuracy satisfactory enough to be tested in the facility [14]. The air speed in the tunnel covered the whole range of stratospheric airship experimental airspeeds. The maximum speed reached was 16 m/s. The turbulence level in the test section was around 0.1% - 0.5%. The sketch of open circuit wind tunnel was shown in Fig. 1. The sketch of the experimental setup was shown in Fig. 2.

Six-components strain gage balances were used for propeller thrust and torque measurements. Each of propellers was connected to a balance which was linked to a collector ring at the other end. The collector ring played an important role during the measuring process to transmit the electrical signals from the balance with high rotational speed to the data acquisition system. The data acquisition system was responsible for transferring the electrical signals to the thrust and torque information. The introductions of data acquisition system were illustrated in reference [14].

Two electric motors were used to drive the propellers. The diameter of motor cross section was smaller than 20% of propeller diameter. Both of the motors were supported by steel stands and installed on the rotation axis of propeller disk. The maximum rotational speed of the motor was 1500 RPM. In order to reduce the influence of supporting objects in the airflow, the fairing was used and the cross section of steel stands was streamline shaped. Figure 3 showed the CRP model with the stands in the wind tunnel.

This paper mainly aimed at analyzing the feasibility

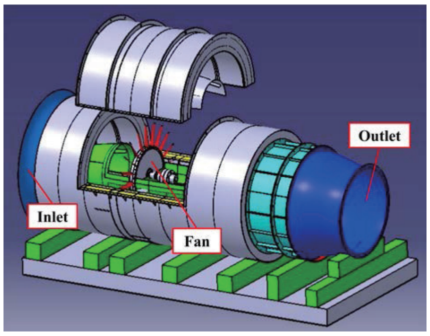

Fig. 1. The sketch of open circuit wind tunnel

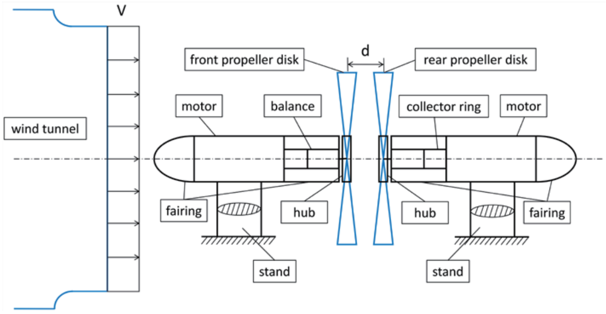

Fig. 2. The sketch of the experimental setup

(a) (b)

Fig. 3. The CRP model with the stands in wind tunnel

DOI: http://dx.doi.org/10.5139/IJASS.2015.16.4.485

of the CRP system to improve the propulsion efficiency of stratospheric airship. Before a definite design method for CRP at low Reynolds number and small advance ratio was developed, the model of a close pair of single-rotating propellers (SRPs) was instead. The two SRPs were exactly the same except for their opposite rotational directions. They were optimum designed by strip theory [15, 16] for stratospheric airship and validated by experiment in accordance with the similarity principle [14, 17]. The propeller models were made of aluminum alloy. The shape parameters of the propeller blade were shown in Fig. 4. The design point and experimental validation of each component of the CRP was introduced in Table 1. The airfoil of the blade elements was S1223, of which the coordinates and force characteristics were shown in [18, 19]. The airfoils were stacked along a straight line passing through their aerodynamic center, as shown in Fig. 5. In the CRP configuration, the spacing *d* between two propellers was fixed at 0.115 m. The RPM of rear propeller was maintained exactly the same as that of front propeller

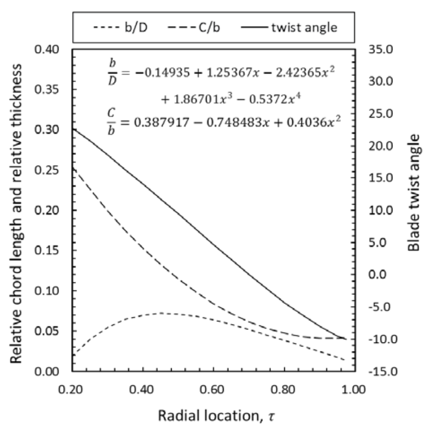

Fig. 4. The shape parameters of the propeller blades (Here *b* is the chord length of the blade, *C* is the thickness and *D* is the diameter of the propeller disk.)

Table 1. The design parameters with experimental validation of each component of the CRP

Parameters	Design Point	Experimental Validation
Altitude, km	20	0
Air Density, kg/m^3	0.08803	1.22505
Air Dynamic viscosity, Pa·s	1.4216	1.7894
Number of Blades	2	2
Diameter, m	6.0	0.75
Blade Element Airfoil	S1223	S1223
Pitch Angle (τ=0.70), deg	28.3	28.3
Advance Speed, m/s	20	14.5
Rotational Speed, RPM	200	1158
Reynolds Number (τ=0.70)	39,000	39,000
Advance Ratio	1.0	1.0
Efficiency, %	73.6	70.7

and the pitch angles of both blades (τ=0.70) were fixed at 28.3 deg.

The testing conditions were introduced in Table 2 in which the Reynolds number of the propeller could be represented by that of a certain blade element. The definition of Reynolds number was described as Eq. (1).

$$\mathrm{Re}_\tau = \frac{\rho b_\tau \sqrt{V^2 + (\tau \pi n D)^2}}{\mu} \quad (1)$$

where τ was proportional radial location of blade element ($\tau = r/R$), Re_τ was Reynolds number of blade element at radial location τ, b_τ was chord length of blade element at radial location τ, and μ was dynamic viscosity coefficient. For example, $Re_{0.7}$ was applied in this paper to describe the Reynolds number of propeller. To achieve a better experimental accuracy every data point was sampled 7 times.

The following parameters were measured in the course of experiment: wind speed in the tunnel, Propeller RPM, thrust, and torque. The wind speed was measured using a differential pressure transmitter with the accuracy of ±0.1 m/s. The RPM of motor was measured by a tachometer with the accuracy of ±5 RPM. Other obtained values, such as power and efficiency, were calculated from those already measured as follows:

Power absorbed by the propeller:

$$P_{absor} = 2 \cdot \pi \cdot n \cdot Q \quad (2)$$

Propeller output power:

$$P_{prop} = T \cdot V \quad (3)$$

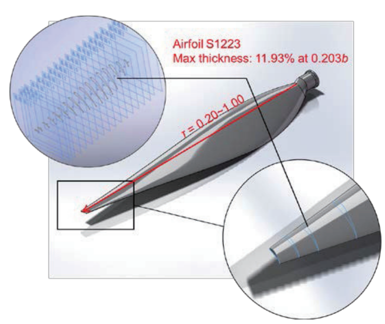

Fig. 5. Construction of the propeller blade elements S1223

Table 2. The testing conditions of the CRP model

Test No.	V, m/s	Range of RPM	Range of $Re_{0.7}$
1	5.0	475~1500	13,000~111,000
2	7.5	600~1500	20,000~112,000
3	10.0	700~1500	27,000~113,000
4	12.5	800~1500	34,000~115,000
5	15.0	1000~1500	40,000~117,000

Propeller efficiency:

$$\eta_{prop} = \frac{P_{prop}}{P_{absor}} \quad (4)$$

where n was number of revolutions per second, Q was torque of propeller, T was thrust of propeller, and V was propeller advance speed or wind speed in experiment. The torque Q necessary in Eq. (2) was measured separately by one balance. Therefore, with front propeller with its motor and stands removed off, it was possible to measure the thrust and torque provided by a half of the propulsion system.

3. Measurement Accuracy Estimation

Duo to several times of experimental data measurements, the Kline's method [20] could be applied in this paper to analyze the measurement uncertainty. The experimental averaged results were determined by Eq. (5). The error of average value was calculated from Eq. (6). The total random error could be expressed as Eq. (8).

$$\bar{x} = \frac{\sum_{i=1}^{m} x_i}{m} \quad (5)$$

$$\Delta x = \sqrt{\frac{\sum \left(x_i - \bar{x}\right)^2}{m-1}} \quad (6)$$

$$\Delta \bar{x} = \frac{\Delta x}{\sqrt{m}} \quad (7)$$

$$\Delta x_c \approx \sqrt{\left(\Delta \bar{x}\right)^2 + \left(\Delta x_p\right)^2} \quad (8)$$

where x was measured value, m was number of measurements, Δx_p was intrinsic error, Δx was mean-square error, $\Delta \bar{x}$ was error of average value, and Δx_c was total random error. Equation (9) was used to calculate the error of functions of many variables:

$$\Delta f \cong \sqrt{\sum_{j=1}^{k} \left(\frac{\partial f}{\partial x_j} \left(\bar{x}\right) \Delta x_{cj} \right)^2} \quad (9)$$

where Δf was error of the function of many variables. Usually, some non-dimensional parameters as follows (Eqs. (10) to (12)) were always applied to describe the performance of propeller.

Advance ratio:

$$J = \frac{V}{nD} \quad (10)$$

Propeller thrust coefficient:

$$C_T = \frac{T}{\rho n^2 D^4} \quad (11)$$

Absorbed power coefficient:

$$C_P = \frac{P_{absor}}{\rho n^3 D^5} \quad (12)$$

where D was propeller diameter and ρ was air density. According to Eq. (4), the propeller efficiency also could be described using the above non-dimensional coefficients, as Eq. (13).

$$\eta_{prop} = \frac{P_{prop}}{P_{absor}} = \frac{TV}{P_{absor}} = J \cdot \frac{C_T}{C_P} \quad (13)$$

Upon the application of the aforementioned estimation procedure of measurement error, the accuracy of propeller non-dimensional parameters was obtained (see Table 3).

4. Results and Discussions

The aerodynamic performance of propeller is always illustrated through figures with non-dimensional aerodynamic coefficients as functions of advance ratio. As tested in accordance with the similarity principle, the non-dimensional parameters of wind-tunnel models would be equal to the prototype at high altitude [17]. Except for the testing conditions in Table 2, the experiment of the standard propeller (SRP configuration) has also been conducted in this paper as a comparison.

Figure 6 shows the aerodynamic parameters of the front and rear propellers with various wind speeds. It can be found that the thrust and power coefficients reduce with the increasing of advance ratio, while the propeller efficiency improves firstly and then reduces regardless of the wind speeds. The peak efficiency can be gained near the designed advance ratio J=1.0. Sometimes the variation of power coefficient is oscillatory (the front propeller at V=7.5 m/s). It might result from the complex combination effects mixed with Reynolds numbers and advance ratios. Another phenomenon can be obtained is different from conventional high-speed aircraft CRPs at relatively low altitude, the thrust and power coefficients are highly dependent on wind speed. However, the Reynolds number is proportional to the wind speed (see Eq. (1)). So it also can be concluded that the non-dimensional parameters increase with the increasing of Reynolds number. The effect of Reynolds number is significant until it reaches high enough value beyond which the parameters become Reynolds number independent.

DOI: http://dx.doi.org/10.5139/IJASS.2015.16.4.485

A blade of a propeller can be treated as a rotating wing that consists of a series of blade elements with angles of attack along the radial location [15]. It is all known that, for a blade element airfoil, the force coefficients under low-speed free flow are related to not only the angle of attack but also the Reynolds number [21]. And then the force coefficients are just related to angle of attack as the Reynolds number is high enough. Under high-speed free flow (usually close to sound speed), the performance of airfoil is affected by Mach number additionally. Similarly, the performance of propeller on the conventional aircraft is determined by advance ratio, pitch angle, and Mach number at blade tip instead of Reynolds number because of the high operation speed and low operation altitude. In terms of the CRP for stratospheric airships, Mach number around the blades is usually under 0.3 so its effect always can be neglected. Instead, the Reynolds number is extremely low at high altitude (see Table 2) so its effects become dominant. This is the reason why the performance of CRP influenced significantly by the Reynolds number according to worse blade element characteristics at low Reynolds number. Judging from Fig. 6, the high efficiency area of the given CRP locates at advance ratio varying from 0.8 to 1.2. The highest peak efficiency of the front propeller is only 69% whereas the rear propeller reaches close to 90%.

As aforementioned description, the performance of CRPs for stratospheric airships should be discussed with a certain Reynolds number which the airship is flying at. Accordingly, it is difficult to analyze the advantages of the CRP with a wide range of various Reynolds number from

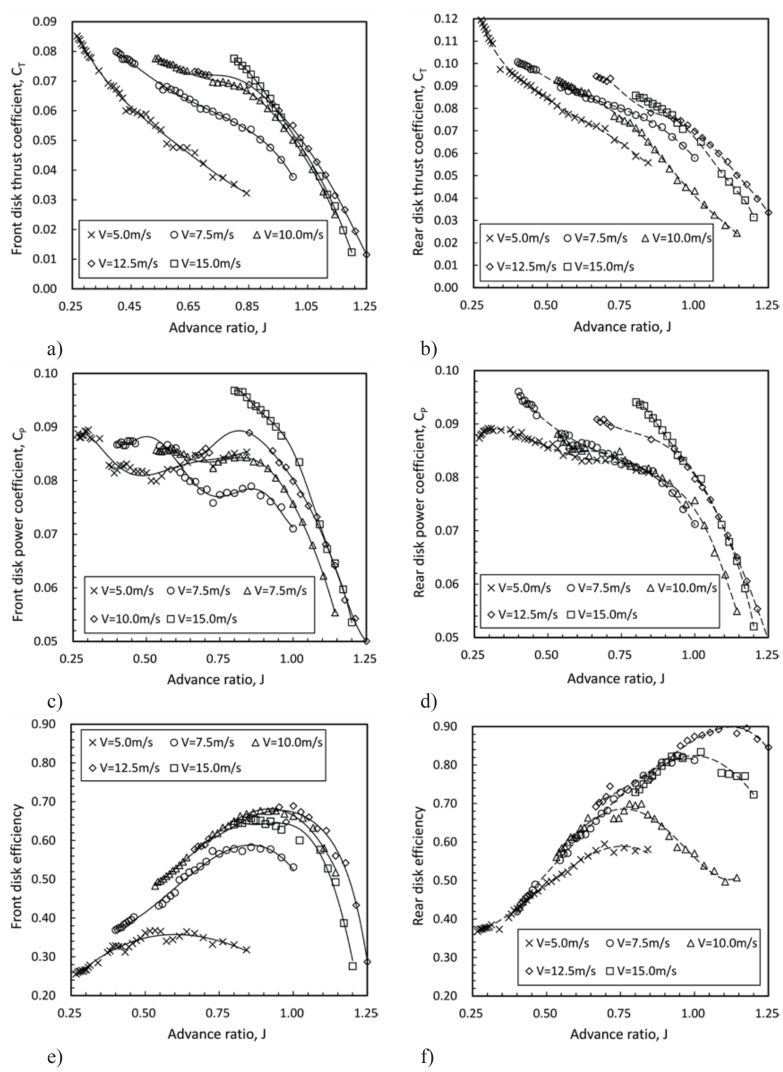

Fig. 6. The aerodynamic parameters of front and rear propellers, a) thrust coefficient of front propeller, b) thrust coefficient of rear propeller, c) absorbed power coefficient of front propeller, d) absorbed power coefficient of rear propeller, e) efficiency of front propeller, f) efficiency of rear propeller

13,000 to 117,000. In order to analyze the performance differences between CRPs and standard propellers, reorder all the experimental data in Fig. 6 as the value of Reynolds number (τ=0.70), and then select the data at a narrow range of Reynolds number (τ=0.70) values from 85,000 to 115,000 to form a figure as a function of advance ratio (see Fig. 7). This comparison between CRPs and standard propellers yields very interesting conclusions.

The differences between the front or rear propeller and the standard propeller prove the existence of interference between front and rear propellers. Compared with two-blade standard propeller, the thrust coefficient of front propeller slightly reduces. Meanwhile, the absorbing power coefficient of the front propeller has no obvious variation. This results in the slightly decrease in the front propeller efficiency. On the contrary, the thrust coefficient of the rear propeller significantly increases due to the interference

Table 3. The total random error of measured data

V, m/s	J	Total Random Error, %		
		T	V	η_{prop}
5.0	0.604	1.78	1.62	3.21
	0.906	1.24	2.18	3.25
10.0	0.604	0.95	0.97	2.63
	0.906	0.92	1.37	2.77
	1.171	3.29	1.96	2.82
15.0	0.604	0.76	0.80	2.13
	0.906	0.78	0.76	2.49
	1.171	2.98	1.10	2.36

by the front propeller. This causes a great increase in the rear propeller efficiency. This phenomenon just proves a conclusion of previous investigations [22] which suggests swirl energy generated by the front propeller is recovered by the rear propeller in the CRP configuration. In a view of the overall CRP, as the improvement of the rear propeller efficiency sufficiently makes up the loss of the front propeller, the efficiency of the CRP is higher than the standard propeller.

Table 4 gives some quantifiable results of the experiment in this paper. A pair of isolate standard propellers seem to provide comparable thrust as the CRP configuration. However, as can be seen from the comparison given in Table 4, the thrust coefficient of the CRP is more than twice of the standard propeller at a given wind speed, whereas the absorbed power coefficient is almost exactly twice as high as that in a standard one. The efficiency of stratospheric airship CRP is about 4 to 8 percent greater as compared to a standard propeller. It indicates the CRP system is better than standard propellers. The application of the CRP system can make the stratospheric airship propulsion more efficient. That is the main purpose the whole research aimed at.

5. Conclusions

Main purposes of this paper have been achieved. The

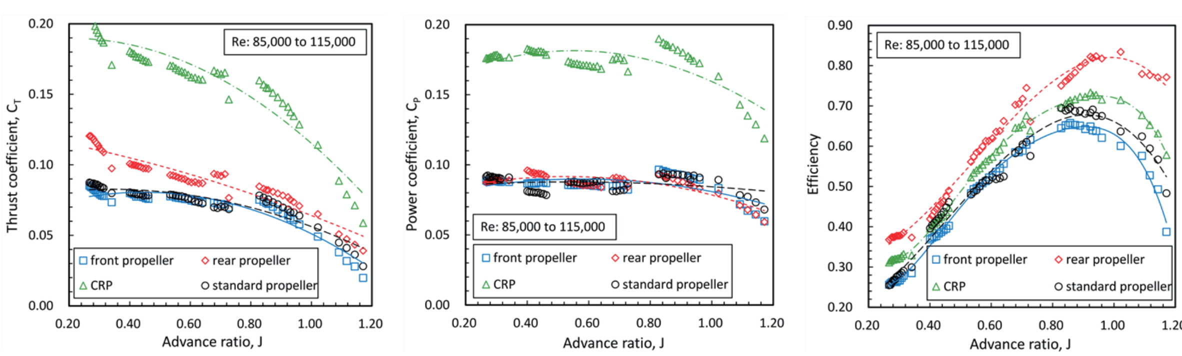

(a) (b) (c)

Fig. 7. The aerodynamic parameters of propellers at $Re_{0.7}$=85,000 ~115,000, a) thrust coefficient, b) absorbed power coefficient, c) propeller efficiency

Table 4. Comparison between aerodynamic coefficients measured in the experiment for CRP and a standard propeller

J	Standard Propeller			CRP			Comparison		
	C_{T1}	C_{P1}	η_1	C_{T2}	C_{P2}	η_2	C_{T2}/C_{T1}	C_{P2}/C_{P1}	η_2-η_1
0.302	0.0841	0.0902	0.2813	0.1902	0.1784	0.3219	2.262	1.978	0.0406
0.533	0.0789	0.0877	0.4798	0.1703	0.1739	0.5228	2.158	1.983	0.0430
0.702	0.0704	0.0817	0.6041	0.1643	0.1761	0.6548	2.334	2.155	0.0507
0.906	0.0697	0.0928	0.6808	0.1438	0.1802	0.7227	2.063	1.942	0.0419
1.021	0.0556	0.0892	0.6365	0.1142	0.1631	0.7146	2.054	1.828	0.0781

DOI: http://dx.doi.org/10.5139/IJASS.2015.16.4.485

feasibility of stratospheric airship contra-rotating propellers has been assessed and the performance of propellers has been investigated.

According to the wind tunnel tests, at relatively low Reynolds number, the aerodynamic performance of propellers is different with variation of Reynolds number. So the contra-rotating propeller design has to be considered at the Reynolds number it really will be flying at.

Moreover, the existence of interference between front and rear propeller is proved by comparison between contra-rotating and standard propellers. The rear propeller recovers the energy of swirl airflow in the slipstream of front propeller, which would cause a great addition of rear propeller efficiency. Therefore, at the same Reynolds number, the efficiency of contra-rotating propeller achieved appears to be a few percent greater than that of a standard conventional propulsion system. It indicates contra-rotating propellers would be an efficient means to improve the performance of stratospheric airship propulsion system.

Acknowledgement

This work was supported by the National Natural Science Foundation of China (Grant No. 11272034), the China-EU Aeronautical Science & Technology Cooperation Project DRAGY.

References

[1] Schmidt, D. K., Stevens, J. and Roney J., "Near-Space Station-Keeping Performance of a Large High-Altitude Notional Airship", *Journal of Aircraft*, Vol. 44, No. 2, 2007, pp. 611-615. DOI: 10.2514/1.24863

[2] Colozza, A., "Initial Feasibility Assessment of a High Altitude Long Endurance Airship", NASA/CR-2003-212724, 2003.

[3] Jamison, L., Sommer, G. S. and Porche, I. R., "High-Altitude Airships for the Future Force Army", Rand Arroyo Center TR-234-A, Santa Monica, CA, 2005.

[4] Moomey E. R., "Technical Feasibility of Loitering Lighter-than-Air Near-Space Maneuvering Vehicles", M.S. Dissertation, U.S. Air Force Inst. Of Technology Rept. ADA437762, Wright-Patterson AFB, OH, March 2005.

[5] Carichner, G. E. and Nicolai, L. M., *Fundamentals of Aircraft and Airship Design (Volume 2: Airship Design and Case Studies)*, AIAA Education Series, AIAA, Reno, VA, 2013, pp. 151-195.

[6] Biermann, D. and Gray, W. H., "Wind-Tunnel Tests of Single-and Dual-Rotating Pusher Propellers Having from Three to Eight Blades", NACA ARR (WR L-359), 1942.

[7] Biermann, D. and Hartman, E. P., "Wind-Tunnel Tests of Four- and Six-Blade Single- and Dual-Rotating Tractor Propellers", NACA Rept. 747, 1942.

[8] Colehour, J. L. and Davenport, F. J., "Analysis of Counter-Rotating Propeller Performance", *AIAA 23rd Aerospace Sciences Meeting*, Reno, Nevada, 1985, AIAA Paper 1985-0005, DOI: 10.2514/6.1985-5

[9] Wainauski, H. S. and Vaczy, C. S., "Aerodynamic Performance of a Counter Rotating Prop-Fan", *AIAA/ASME/SAE/ASEE 22nd Joint Propulsion Conference*, Huntsville, Alabama, 1986, AIAA Paper 1986-1550, DOI: 10.2514/6.1986-1550

[10] McHugh, J. G. and Pepper, E., "The Characteristics of Two Model Six-Blade Counterrotating Pusher Propellers of Conventional and Improved Aerodynamic Design", NACA ARR (WR L-404), 1942.

[11] Gray, W. H., "Wind Tunnel Test of Dual-Rotating Propellers with Systematic Differences in Number of Blades, Blade Setting and Rotational Speed of Front and Rear Propellers", NACA ARR L4E22 (WR L-80), 1944.

[12] Shin, H., Whitfield, C. E. and Wisler, D. C., "Rotor-Rotor Interaction for Counter-Rotating Fans, Part 1: Three-Dimensional Flowfield Measurements", *AIAA Journal*, Vol. 32, No. 11, 1994, pp. 2224-2233. DOI: 10.2514/3.12281

[13] Stürmer, A., Marquez Gutierrez, C. O., Roosenboom, E. W. M., Schröder, A., Geisler, R., Pallek, D., Agocs, J. and Neitzke, K., "Experimental and Numerical Investigation of a Contra Rotating Open-Rotor Flowfield", *Journal of Aircraft*, Vol. 49, No. 6, 2012, pp. 1868-1877. DOI 10.2514/1.C031698

[14] Ma, R., "Design Technology Study on the High-Efficiency Propeller of the Low Dynamic Vehicles in Stratosphere", Ph.D. Dissertation, School of Aeronautic Science and Engineering, Beihang University, Beijing, China, 2010.

[15] Wald, Q. R., "The Aerodynamics of Propellers", *Progress in Aerospace Sciences*, Vol. 42, No. 2, 2006, pp. 85-128. DOI: 10.1016/j.paerosci.2006.04.001

[16] Okulov, V. L., Sørensen, J. N. and Wood, D. H., "The rotor theories by Professor Joukowsky: Vortex theories", *Progress in Aerospace Sciences*, Vol. 73, 2015, pp. 19-46. DOI: 10.1016/j.paerosci.2014.10.002

[17] Liu, P., Ma, L., Duan, Z. and Ma, R., "Study and Verification on Similarity Theory for Propellers of Stratospheric Airships", *Journal of Beijing University of Aeronautics and Astronautics*, Vol. 38, No. 7, 2012, pp. 957-961.

[18] Selig, M. S., Lyon, C. A., Giguere, P., Ninham, C. P. and Guglielmo, J. J., *Summary of Low-Speed Airfoil Data (Volume*

2), SoarTech Publications, Virginia Beach, Virginia, 1996.

[19] Selig, M. S. and Guglielmo, J. J., "High-Lift Low Reynolds Number Airfoil Design", *Journal of Aircraft*, Vol. 34, No. 1, 1997, pp. 72-79. DOI: 10.2514/2.2137

[20] Kline, S. J., "The Purpose of Uncertainty Analysis," *Journal of Fluids Engineering*, Vol. 107, No. 2, June 1985, pp. 153-160. DOI: 10.1115/1.3242449

[21] Anyoji, M., Nonomura, T., Aono, H., Oyama, A. and Fujii, K., "Computational and Experimental Analysis of a High-Performance Airfoil Under Low-Reynolds-Number Flow Condition", *Journal of Aircraft*, Vol. 51, No. 6, 2014, pp. 1864-1872. DOI: 10.2514/1.c032553

[22] Mieloszyk, J., Galinski, C., Piechna, J. and Brzozowski, J., "Contra-Rotating Propeller for Fixed Wing MAV: Part 2", *Aircraft Engineering and Aerospace Technology*, Vol. 85, No. 4, 2013, pp. 316-325. DOI: 10.1108/AEAT-Jan-2012-0009